Exhumation history of orogenic highlands determined by detrital fission-track thermochronology

JOHN I. GARVER[1], MARK T. BRANDON[2], MARY RODEN-TICE[3] & PETER J. J. KAMP[4]

[1]*Geology Department, Union College, Schenectady, NY 12308–2311, USA (e-mail: garverj@union.edu)*

[2]*Department of Geology and Geophysics, Yale University, P.O. Box 208109, 210 Whitney Avenue, New Haven, CT 06520–8109, USA*

[3]*Earth and Environmental Sciences, State University of New York at Plattsburgh, Plattsburgh, NY, 12901, USA*

[4]*Geochronology Research Unit, Earth Sciences Department, University of Waikato, Private Bag 3105, Hamilton, New Zealand*

Abstract: A relatively new field in provenance analysis is detrital fission-track thermochronology which utilizes grain ages from sediment shed off an orogen to elucidate its exhumational history. Four examples highlight the approach and usefulness of the technique. (1) Fission-track grain age (FTGA) distribution of apatite from modern sediment of the Bergell region of the Italian Alps corresponds to ages obtained from bedrock studies. Two distinct peak-age populations at 14.8 Ma and 19.8 Ma give calculated erosion rates identical to *in situ* bedrock. (2) Zircon FTGA distribution from the modern Indus River in Pakistan is used to estimate the mean erosion rate for the Indus River drainage basin to be about 560 m Ma^{-1}, but locally it is in excess of 1000 m Ma^{-1}. (3) FTGA distribution of detrital apatite and zircon from the Tofino basin records exhumation of the Coast Mountains in the Canadian Cordillera. Comparison of detrital zircon and apatite FT ages gives exhumation rates of *c.* 200 m Ma^{-1} during the interval between *c.* 34 and 54 Ma, but higher rates (*c.* 1500 m Ma^{-1}) at *c.* 56 Ma. (4) FTGA analysis of apatite grain ages from a young basin flanking Fiordland in New Zealand indicates that removal of cover strata was followed by profound exhumation at *c.* 30 Ma, which corresponds to plate reorganization at this time. Exhumation rates at the onset of exhumation were *c.* 2000–5000 m Ma^{-1}. These studies outline the technique of detrital FTGA applied to exhumation studies and highlight practical considerations: (1) well-dated, stratigraphically coordinated suites of samples that span the exhumation event provide the best long-term record; (2) strata from the basin perimeter are the most likely to retain unreset detrital ages; (3) the removal of 'cover rocks' precedes exhumation of deeply buried rocks, which retain a thermal signal of the exhumation event; (4) steady-state exhumation produces peak ages that progressively young with time and have a constant lag time; (5) same-sample comparison of zircon and apatite peak ages is best in sequences with high-uranium apatite grains (>50 ppm), and peak-ages statistics can be improved by counting numerous apatite grains (>100).

Orogenic sediments provide an integrated view of the tectonic and climatic factors that shape the evolution of mountainous regions. Stratigraphers and sedimentologists have spent considerable effort using the provenance of sediments to understand the evolution of adjacent source regions. A relatively new field in provenance analysis is detrital fission-track thermochronology, which utilizes the fission-track ages of single detrital grains to identify and characterize the source region and also to quantify its thermochronological evolution.

Unravelling the long-term evolution of mountain systems requires a detailed understanding of the relationship between uplift, erosion, and deposition. One approach has been to apply different mineral thermochronometers to bedrock samples for eroded landscapes, or to sedimentary detritus that collects in nearby basin sequences. Studies using bedrock exposures are limited to only those rocks exposed at the surface and therefore provide only limited information about the entire evolution of that orogenic system because overlying rock, which presumably had a record of earlier thermotectonic events, has been stripped away and lost to adjacent basins. On the other hand, sedimentary basins that surround orogenic belts contain an easily accessible, long-term orogenic record, but the evidence is fragmentary and needs to be

GARVER, J. I., BRANDON, M. T., RODEN-TICE, M. & KAMP, P. J. J. 1999. Exhumation history of orogenic highlands determined by detrital fission-track thermochronology. *In:* RING, U., BRANDON, M. T., LISTER, G. S. & WILLETT, S. D. (eds) *Exhumation Processes: Normal Faulting, Ductile Flow and Erosion.* Geological Society, London, Special Publications, **154,** 283–304.

reassembled. Sediments, however, commonly provide the only long-term record for an evolving orogenic system. In detrital FT thermochronology, the goal is to examine stratigraphic sequences, and relate upsection changes in FT grain ages to the thermal evolution of the source region. Another similar approach has been laser-probe $^{40}Ar/^{39}Ar$ dating of detrital potassium-bearing minerals such as biotite, muscovite, amphibole, and feldspar (e.g. Horstmann 1987; Cohen *et al.* 1990; Copeland and Harrison 1990; Copeland *et al.* 1990; Grist *et al.* 1990; Renne *et al.* 1990; Turner *et al.* 1996; Dallmeyer *et al.* 1997).

FT dating of common detrital uranium-bearing minerals such as apatite, zircon and sphene has been used for some time now in provenance analysis, stratigraphic correlation, and dating sediments (McGoldrick & Gleadow 1977; Wagner *et al.* 1979; Zeitler *et al.* 1982, 1986; Hurford *et al.*, 1984; Yim *et al.*, 1985; Baldwin *et al.* 1986; Kowallis *et al.* 1986; Naeser *et al.* 1987, 1989; Cerveny *et al.* 1988; Garver 1988; Vance 1989; Corrigan & Crowley 1990; Brandon & Vance 1992; Hasebe *et al.* 1993; Maranville 1993; Garver & Brandon 1994*a*,*b*; Frisbee 1995; Carter 1996; Dunkl *et al.* 1996; Tagami & Dumitru 1996; Pereira *et al.* 1996; Rohrman *et al.* 1996). A more recent development has been to use FT ages of detrital zircon or apatite from stratigraphic sequences to reconstruct source region exhumation (Garver *et al.* 1993; Brown *et al.* 1994; Garver & Brandon 1994b; Johnson & Lonergan 1996; Rohrman & Andriessen 1996; Rohrman *et al.* 1996). It seems clear that this approach holds great promise for understanding the long-term relationship between tectonics, topography, climate, erosion, and sedimentation in orogenic settings.

Generally, source regions have distinct thermotectonic signatures, which are clearly retained in the erosional detritus. In our experience, most source regions in orogenic settings can be characterized as one of three important thermotectonic regimes: (a) source regions exhumed by progressive erosion; (b) source regions unroofed by tectonic processes; (c) source regions characterized by high geothermal gradients and active volcanism. The first case, which is highlighted in this paper, involves a source region that evolves through progressive erosion. In this case, rocks move upward in the crust through a closure isotherm, the FT clock starts, and eventually the rock reaches the surface, is eroded and the detritus is deposited in adjacent basins. All of these cases have distinct FT grain age (FTGA) patterns.

This paper reviews the basic concepts and techniques of detrital FT thermochronology, and highlights the strategy and implementation of this approach by looking at both the zircon and apatite systems. Then, to illustrate these concepts, we provide examples, from a small drainage basin in the centre of the Italian Alps, the Indus River, which drains the western Himalayan Mountains, a basin flanking the Coast Mountains of western Canada, and a basin flanking the Fiordland block in southern New Zealand.

Erosion, transport, and deposition

In a simple setting, erosional exhumation progressively unroofs rocks in a source area and the sediment is shed into an adjacent basin (Fig. 1a and b). During exhumation, a rock passes through the closure temperature T_c and closure depth Z_c for the isotopic system of interest to the surface (which has an average temperature of T_s). Once at the surface, it is then eroded at time t_e, transported, and deposited at t_d in adjacent sedimentary basins. A critical aspect of this system is the ΔT for the sample, which is given by $T_c - T_s$. Sediment storage for a certain length of time ($t_e - t_d$) may occur sometime between erosion (t_e) and deposition (t_d). Ultimately, we are interested in determining the effective exhumation rate of the system from a well-dated stratigraphic sequence ($\dot{\varepsilon}$ in m Ma^{-1}). To do this, several important variables need to be estimated including, most importantly, the geothermal gradient (G) at the time of closure (t_c). Both of the variables are difficult to quantify accurately and as a result are the main limiting factors in using detrital FTGA analysis to estimate exhumation.

One can use FT ages from bedrock samples to estimate long-term exhumation rates. Use of this approach is routine in the FT analysis of bedrock samples, especially suites of samples from mountainous regions (see review by Wagner & Van den haute (1992)). A common approach is to assume a linear geotherm and a specific closure temperature. In this case, the average exhumation rate is given by the following equation:

$$\dot{\varepsilon}_m = [(T_c - T_s)/G] / \Delta t \quad (1)$$

where $\dot{\varepsilon}_m$ is a model exhumation rate, $\Delta t = t_e - t_c$ which is the lag time, and G is the geothermal gradient.

In detrital FTGA spectra, essentially the same approach is used for distinct grain-age populations. These populations are referred to as component 'populations' or 'peaks' and they are defined by either a Gaussian or binomial fit

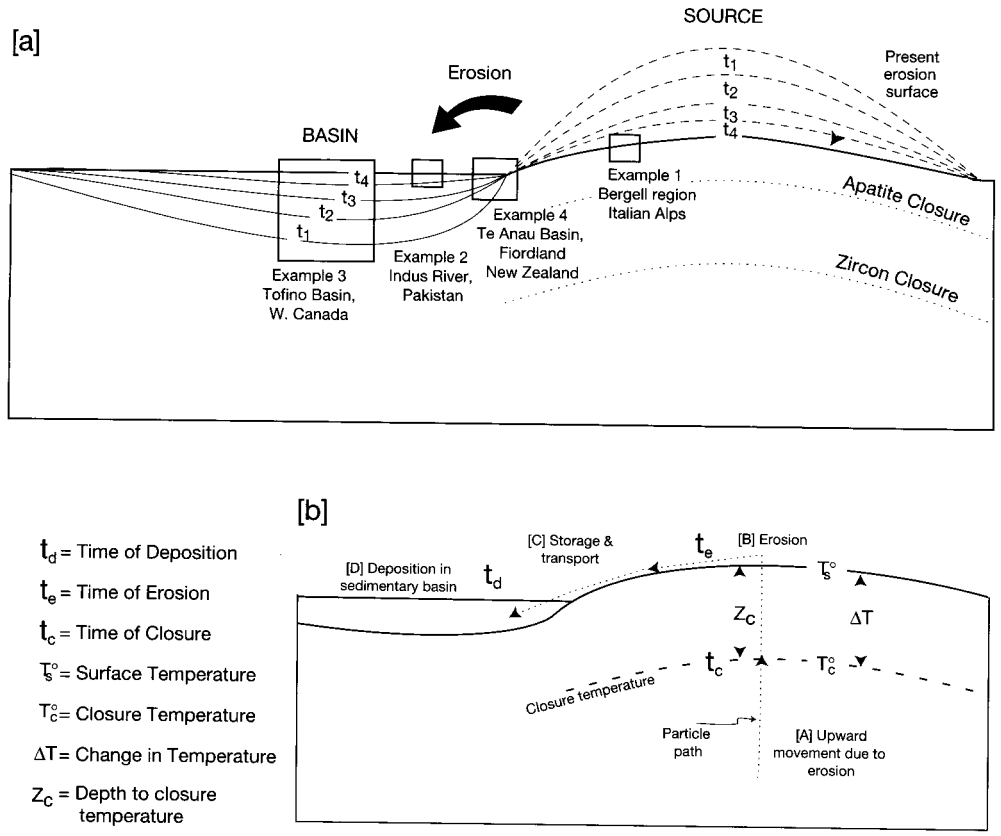

Fig. 1. Schematic representation of an idealized erosion of a mountain range and the variables used in FTGA calculations. (**a**) Schematic diagram showing development of an exhumational sequence through time. In this simple case, a source is progressively unroofed and the sedimentary detritus is deposited in an adjacent basin. It should be noted that the thickness of the strata varies in the basin, but locally, once the strata are thick enough, they enter the apatite annealing zone and in terms of FT ages, the provenance information in the apatite is lost. Time slices (t_1–t_4) correspond to four progressive and continuous intervals of erosion and deposition in which initial deepening in the basin was followed by basin infilling and erosional decay. The examples in this paper come from the different areas of the system denoted in the figure. (**b**) Variables used in model exhumation calculations. It should be noted that a particular rock follows the dotted lined marked as 'particle path'. As the rock moves upward toward the surface, it passed the critical closure isotherm and fission tracks begin to accumulate. Through exhumation of the region, that rock then passes upwards to the surface some distance Z'_c which is estimated by making assumptions about the closure temperature, surface temperature and the geothermal gradient. The rock is then eroded and deposited in an adjacent basin, a part of the journey that is inferred to be geologically instantaneous.

to the composite dataset (Galbraith & Green 1990; Brandon 1992, 1996). For example, let us assume that a young population or 'peak' of apatite grain ages (see section on 'peak-fitting') P_1 from Recent river sediment occurs at 14 Ma. In this case the lag time or Δt in equation (1) is given by $t_d - t_c$, which represents the time between passage through the partial annealing zone (PAZ) and deposition.

For simplicity, it should be noted that for detrital samples, lag time includes not only the time from closure to the surface, but also the time needed to erode and transport the sediment into nearby sedimentary basins, but we suspect that the transport time is fast in rapidly eroding mountain belts (Brandon & Vance 1992). We take the approach here that when viewed at the scale of the entire drainage system, sediment storage is part of the erosion process. In other words, the material has not been eroded from the drainage system until it has moved out of the entire system. This view becomes less

credible when the distance between the erosional drainage and the sampled basinal setting become large. With large distances, there is a greater probability that transient basins may have existed along that transport path.

FT dating

Naturally formed fission tracks in common minerals are generally the result of fission of ^{238}U at a rate of about $10^{-16}a^{-1}$ (see Fleischer *et al.* 1975; Naeser 1976; Wagner & Van den haute 1992). These fission events result in the recoil of two highly charged sub-equal nuclei that create a damage zone in the crystal lattice, which can be easily enlarged by chemical etching and then viewed at high magnification with a microscope.

Annealing of fission tracks is a function of time and temperature. Although the annealing temperatures of apatite and zircon have been studied in the laboratory, difficulty arises when extrapolating these conditions to geologically reasonable conditions (see Wagner & Van den haute 1992). Resetting and closure of fission-track ages are commonly approximated using the concepts of a PAZ and an effective closure temperature, which are summarized in Fig. 2. The PAZ describes the temperature range in which existing fission tracks are partially annealed. In practice, the upper and lower limits of the PAZ can be defined by the temperatures needed to cause 10 and 90% annealing after a specified period of time (Fig. 2a). For natural α-damaged zircon, the PAZ is about 180–240°C for heating times of between 1 and 25 Ma, whereas for fluorapatite, it is about 40–120°C. Composition and radiation damage can influence annealing behaviour. For instance, fission tracks will persist to higher temperatures in zircons with little or no α-radiation damage (Kasuya & Naeser 1988) or in apatites with higher Cl contents (Green *et al.* 1985). Thus, it is important to keep these factors in mind when interpreting fission-track ages. We are particularly concerned with the lower-temperature side of the PAZ, which determines where grain ages start to reset. Assuming a typical continental geotherm of 25°C km^{-1} and an average surface temperature of *c.* 10°C, we would expect to preserve unreset detrital grain ages at depths less than 1.2 km for fluorapatite and less than about 7 km for α-damaged zircons.

Closure of the fission-track system occurs as a sample cools through the PAZ. None the less, it is useful to define an effective closure temperature T_c, which is the temperature of the sample at the time indicated by the fission-track age. If

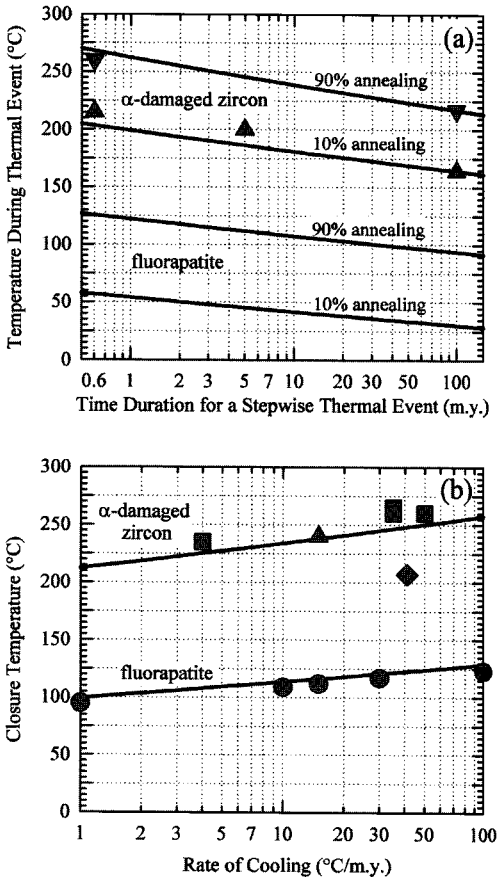

Fig. 2. The thermal stability and T_c for fission tracks in fluorapatite (Durango) and natural α-damaged zircon (from Brandon *et al.* 1998). (**a**) The partial annealing zones (PAZs) are represented by the 10 and 90% annealing isopleths, which have an Arrhenius-like relationship. (**b**) T_c is estimated for monotonic cooling through the PAZ at an approximately constant cooling rate. Symbols show other estimates for T_c: circles, predictions of a track-length annealing model; triangles, comparison of zircon FT ages and biotite K/Ar ages; squares, comparisons of zircon FT ages with $^{40}Ar/^{39}Ar$ K-feldspar ages; diamonds, comparison of zircon FT ages with apatite FT and K/Ar biotite ages (see Brandon *et al.* (1998) for complete discussion).

one can assume that the sample cooled through the PAZ at an approximately steady rate, then T_c can be calculated as a function of cooling rate (Fig. 2b). For typical geological cooling rates of 1–30°C Ma^{-1}, the T_c for fluorapatite is about 100–120°C, and for α-damaged zircon about 215–240°C. Laboratory experiments by Yamada *et al.* (1995) suggest that T_c for zircon might be

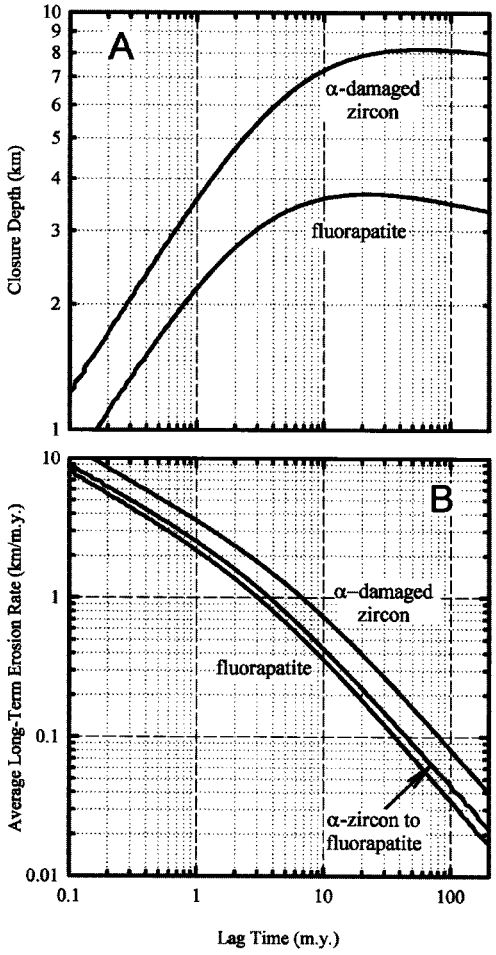

Fig. 3. The lag time shown as a function of closure depth and average long-term erosion rates. (**a**) Relationship between apatite and zircon closure depth with lag time. The lines makes approximate corrections for changes in closure depth caused by displacement of isotherms and by changes in cooling rates, both of which are a function of exhumation rates. (**b**) Calculations of averaged erosion rates and lag time. The influence of fast erosion rates on the thermal profile can be seen at lag time of about 5 Ma, below which correction must be made for the advection of heat by erosion. The closure depth for long lag times, takes on a constant value of *c.* 3 km for apatite with $t > 10$ Ma. and *c.* 6.5 km for zircon with $t > 20$ Ma (see Brandon *et al.* 1998). The relationship between cooling rate and closure temperature was modelled using the equation of Dodson (1979) with values reported by Brandon & Vance (1992) and Brandon *et al.* (1998). The thermal profile is specified using the solution for steady-state erosion given by Stüwe *et al.* (1994), which assumes a constant erosion rate and fixed temperatures at the base and top of an eroding infinite layer. For the Himalayan example shown in this paper, the layer was assumed to be 30 km thick and the base and top were held at 910°C and 10°C, which implies an initial linear thermal gradient of *c.*30°C km^{-1}. The model results are not very sensitive to the thickness of the layer for thicknesses greater than *c.*20 km. A lower thermal gradient or lower surface temperature will result in a deeper closure depth, all other factors being equal.

50–100°C greater than cited here, but this result is inconsistent with other estimates (see comparisons in Fig. 2). Brandon *et al.* (1998) have reviewed this problem, and suggested that the anomalously high thermal stability observed by Yamada *et al.* (1995) would be consistent for zircons with low α-radiation damage. The amount of α damage present in the zircons studied by Yamada *et al.* (1995) is not known.

In most cases, we are actually interested in estimating the closure depth Z_c (Fig. 3). The closure depth is a function of the geotherm and the rate of cooling, both of which are directly affected by the exhumation process. Brandon *et al.* (1998) proposed an approximate method for estimating closure depth using a one-dimensional steady-state model where erosion at the surface is balanced by accretion at depth. The model assumes that temperatures at the base and surface of a one-dimensional layer are maintained fixed at their initial values. These fixed values can be viewed as describing the initial geotherm (i.e. the steady-state thermal profile before the onset of exhumation). The solution of this model for fission-track closure is not strongly dependent on the layer thickness so long as the thickness is greater than 20 km. The model assumes that the erosion rate has been operating for long enough for the thermal profile to reach a steady-state configuration, which usually requires several millions of years to occur (see Brandon *et al.* (1998) for details). A faster erosion rate will cause isotherms to migrate closer to the surface, but it will also result in a faster cooling rate.

An important aspect of the thermal annealing of apatite is that tracks are progressively shortened while in this PAZ, and the track length distribution can be used qualitatively to assess the rate of cooling through this zone (Gleadow *et al.* 1986). Where cooling is rapid, track lengths of *c.* 14–15 μm are typical.

Apatites that cooled more slowly (i.e. slower exhumation) will tend to have shorter track lengths because they spend more time in the PAZ. Unfortunately, individual apatite grains rarely have more than one or two tracks with appropriate orientations for measurement. In studies of reset samples, this problem is circumvented by collecting track-length measurements from the entire population of grains, but this approach is not appropriate for unreset detrital grain ages because each grain can have a different thermal history. The application of track-length analysis to zircon is still in its developmental phase, but the same problem of low numbers of horizontally confined tracks in single grains will preclude routine use for unreset detrital zircons.

Detrital FT chronology

Unlike a conventional FT age where dated grains from a single source have a common thermal history, FTGA distributions contain many single grain ages, which originated from a variety of thermotectonic source terranes. Several techniques have been proposed to evaluate grain-age distributions, but the Gaussian and binomial peak-fitting methods are the most routinely used (see, e.g. Hurford *et al.* 1984; Seward & Rhodes 1986; Galbraith 1988; Galbraith & Green 1990; Brandon & Vance 1992; Brandon 1996). Here we employ both 'peak-fitting' methods. (Programs used to peak-fit the data in this paper are available by anonymous FTP from: love.geology.yale.edu//pub/brandon/ft/ft_peaks. For Gaussian peak-fitting, individual grain ages are first collectively approximated by a continuous probability density (PD) plot. Next, Gaussian peaks are fitted to the PD, and the sum of the fitted peaks is the model prediction. With an appropriate fit, individual peak ages (P1, P2, etc., in Fig. 4) can then be evaluated. For the binomial peak-fitting technique, populations are estimated directly from the data without the need to generate a PD plot. This latter method has some advantages in that it is based directly on the binomial distribution, which better represents counting statistics for FT dating. It also gives more precise estimates for the uncertainties of peak ages. In practice, however, the two methods commonly give similar results especially when the uncertainty for grain ages is small, which is typically the case for zircon. For both methods, individual fitted peaks have a mean age, size, and peak width (W). It should be noted that the peak width (W) is the relative standard deviation of a peak expressed as a fraction of the peak age.

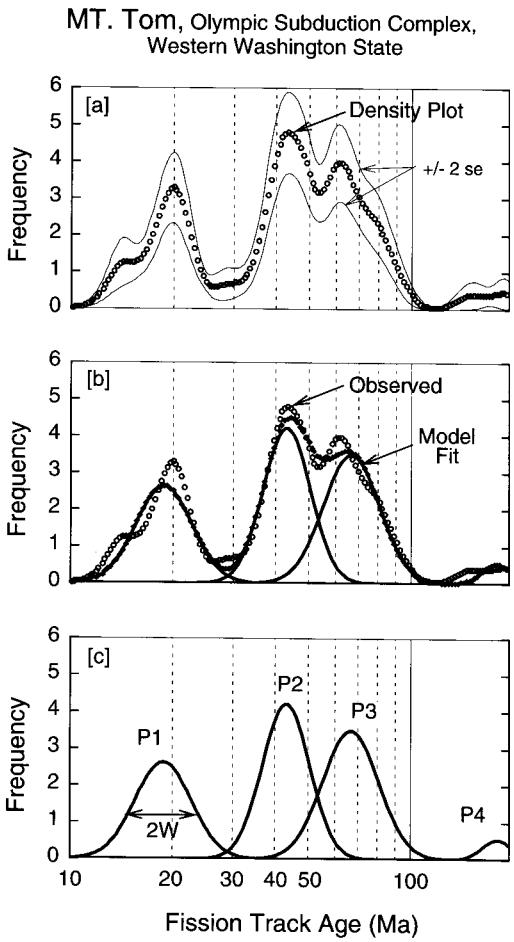

Fig. 4. Composite probability plots and fitted peaks for detrital zircon FT ages from rocks of the Olympic Subduction Complex (western Washington State, USA), shown here to illustrate the general procedure of peak-fitting detrital FT data (data from Brandon & Vance 1992). These rocks are part of the modern accretionary prism to the Cascadia subduction zone, and the zircons in these sandstones were derived from a variety of thermotectonic terranes behind and within the Cascade arc (see Brandon & Vance 1992; Maranville 1993; Frisbee 1995). (**a**) Density plot (±2 SE) showing the observed distribution of all grain ages (n = 50). (**b**) The density plot is then fitted by the Gaussian peak-fitting method (individual peaks) and the modelled fit is maximized to the observed density plot. (**c**) Fitted peak ages are then inferred to represent the age of component populations in the source region (see Brandon (1996) for full explanation).

The two main factors that influence counting statistics and therefore the precision of a single grain-age are uranium concentration and age; both directly affect the number of countable

tracks. Zircon typically ranges between 5 and 4000 ppm uranium (see Speer 1980) and apatite mainly ranges between <1 and 300 ppm but typically falls well below 100 ppm (e.g. Wagner & Van den haute 1992; Dill 1994). For common detrital zircons, the mean uranium concentration is *c.*420 ppm with a mode of *c.* 140 ppm and a range between 100 and 600 ppm (Garver & Brandon in preparation). Therefore, apatite grains range in composition from about 1 to 100 ppm whereas zircon grains typically range from 100 to 500 ppm. This difference in U content results in much lower precision for apatite FT grain ages than that for zircon FT ages.

To illustrate this important effect of uranium variation on FT age, we show a typical distribution of grain ages from the FT reference standard, the Oligocene Fish Canyon Tuff (Fig. 5). In both plots, about 45 typical single-grain ages are plotted. The peak width, W, for apatite is about 0.39, which is much greater than for zircon, where $W = 0.20$. For this example, both FT ages are identical, but the zircon has *c.* 380 ppm U and apatite has *c.*13 ppm (Fig. 5). Given identical cooling ages, less uranium means fewer tracks, which results in less precise grain ages. Thus, high U concentrations are needed (>50 ppm) if apatite is to be used for detrital geochronological study. Our experience suggests that apatite suites from evolved continental crustal blocks tend to have higher uranium concentrations and are better suited for exhumation studies.

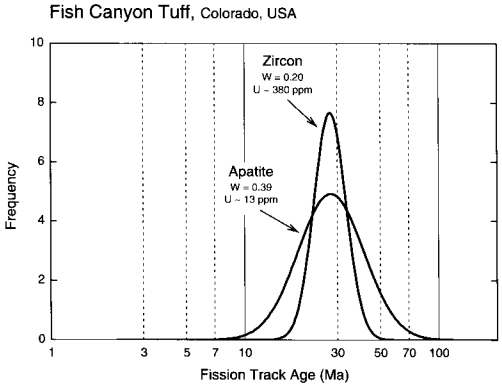

Fig. 5. Plot showing the probability distribution of zircon and apatite grain ages determined by fission-track dating for the 27.9 ± 0.3 Ma Fish Canyon Tuff age standard from Southfork, Colorado (Naeser *et al.* 1981). Minerals from this quickly cooled welded tuff are commonly used as an age standard in fission-track dating and in other geochronological techniques. For both zircon and apatite, *c.* 45 grains are used to construct the plot. It should be noted that the peak is about two times wider for the apatite compared with the zircon, with the contrast ascribed to large differences in uranium concentrations between the two minerals. The lower precision of apatite is typical in most detrital suites, and as a result, apatite is less useful for provenance analysis, especially when the uranium concentration falls below *c.* 50 ppm.

Examples of detrital FT geochronology

In these examples, we show how detrital FTGA distributions can be used to study exhumation of mountainous source regions. In outlining these four cases, we pose several logical questions for the reader to consider: (1) Does the method faithfully capture the cooling ages of bedrock in a drainage basin? (2) Can the cooling ages be applied to understanding the exhumation of an orogenic system? (3) What problems, assumptions, and limitations are encountered? (4) Can detrital FTGA analysis be used to evaluate the temporal evolution of exhumation by using stratigraphically coordinated samples? (5) What approaches are most fruitful and what problems are encountered?

Modern river sediment shed from the Bergell region, Central European Alps

In this first example, we show how FT grain ages from a small modern drainage reflect cooling in the bedrock as independently determined from other studies (Fig. 6). Sediment was collected from a small river near the town of Novate in northernmost Italy near Lake Como to the south and the border between Italy and Switzerland to the north. The upstream drainage is entirely underlain by the Bergell pluton and adjacent country rocks, and it was chosen because the area has a very well-constrained thermal history representative of this part of the Alpine system. In this example we are interested in establishing the FTGA distribution of sediment with a well-defined provenance and thermal history. One hundred and fourteen grains with moderate to high uranium concentrations (mean of 58 ppm, but ranging between 50 and 200 ppm) define two distinct peak ages at 14.8 Ma and 19.8 Ma (Table 1; a full set of fission-track data is available from the Society Library and from the British Library Document Supply Centre, Boston Spa, Wetherby, West Yorkshire LS23 7BQ, UK, as Supplementary Publication No. SUP 18128 (10 pp.)).

The collision between Africa and the European plate has discontinuously affected rocks in this area from Cretaceous to late Tertiary time;

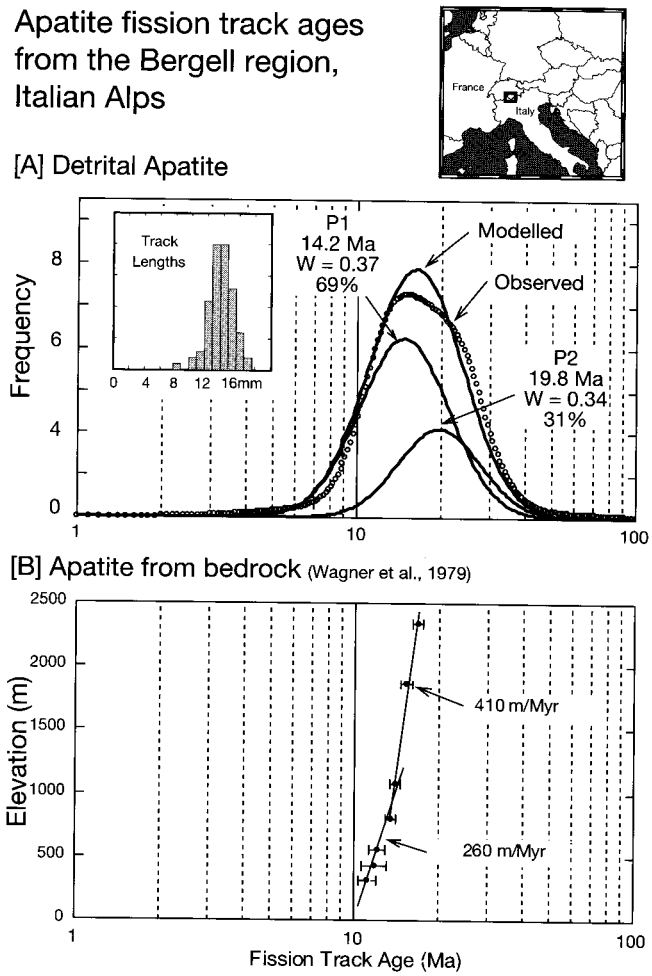

Fig. 6. Fission-track ages from the Bergell region in the Italian Alps: (**a**) detrital FT ages from apatite from river sediment (Table 1); and (**b**) apatite from bedrock samples as reported by Wagner *et al.* (1979). For the detrital sample, all 114 single grain ages were summed to form the probability density (PD) plot (shown as the line defined by small circles). Fitted peaks, P1 and P2, are a best fit using binomial statistics. These peaks sum to a model density plot, which is shown as the continuous line. Wagner *et al.* (1979) recognized two cooling episodes on the age–elevation plot. The first is defined by samples from *c.* 2500 to *c.* 1000 m and gives a exhumation rate of *c.* 410 m Ma^{-1} at a mean age of *c.* 14.2 Ma. The second is defined by samples <1000 m, and gives a exhumation rates of 260 m Ma^{-1} at a mean age of *c.* 11.7 Ma. Inset in (**a**) shows the track-length distribution for the river-sediment apatite. These track lengths (mean 13.98 μm, SD 1.56 μm, $n = 86$) were measured from detrital grains presumably with different thermal histories, but the relatively long mean length of *c.* 14 μm suggests rapid cooling of rocks in the source despite mixing.

here we are interested in the most recent episode of uplift and exhumation. Estimates of long-term exhumation rates for the Central Alps range between about 200 and 400 m Ma^{-1} (see Clark & Jäger 1969; Schaer *et al.* 1975; Wagner *et al.* 1977, 1979; Wagner & Van den haute 1992). The Bergell region of the Central Alps is underlain by the Bergell plutonic suite that intrudes the Penninic Nappes (Schmid *et al.* 1996). Intrusion of the Bergell plutonic suite occurred at about 33–28 Ma, and the suite is notable because some 10 km of magmatic section are enclosed at present (Hansmann 1996; Schmid *et al.* 1996). Apatite fission-track dates from plutonic boulders in Late Oligocene strata of the Po Plain (to the south of the Alps in

Table 1. *Apatite FT peak ages for Bergell river sediments, Italian Alps*

Unit	Age (Ma)	*n*	P1	P2	P3	Track length	*n*
Modern river	0	114	14.2 ± 1.2 W= 0.37 69%	19.8 ± 3.6 W = 0.34 31%	–	13.98 ± 0.1 1.56	86

Apatite grains were mounted in epoxy resin on glass slides and polished to expose internal grain surfaces. The mounts were then etched in 5 M HNO_3 for 20 s at room temperature. With low-uranium mica flakes affixed to the polished and etched mounts, the samples were irradiated at the nuclear reactor at Oregon State University with a nominal fluence of 8×10^{15} neutrons cm^{-2}. Samples were irradiated with the glass dosimeter CN-1 as well, and the Fish Canyon Tuff and Durango age standards. Grains were counted using a Leitz Ortholux microscope at 1250× (100× dry objective, 1.25 tube factor, and 10× oculars). Ages were calculated using a mean weighted $zeta_{CN-1}$ of 107.0 ± 4.5 (± 1 SE; J.I.G.). Peak ages were calculated using the binomial peak-fitting method of Galbraith & Green (1990) (see Brandon 1996). The number of grains in each analysis is represented by '*n*'.

NE Italy) are between 23 and 28 Ma, indicating that the upper levels of the Bergell plutonic suite cooled rapidly after intrusion and was then brought to the surface, eroded, and deposited in flanking basins (Wagner *et al.* 1979; Giger & Hurford 1989). Fission-track dating of bedrock exposures in the Bergell pluton and adjacent rocks elucidate the Miocene exhumation history (Wagner *et al.* 1977, 1979). These data from elevation traverses indicate that the Miocene cooling history of the area was marked by continuous exhumation with rates of *c.* 410 m Ma^{-1} between about 16 and 14 Ma followed by rates of about 260 m Ma^{-1} between about 14 and 11 Ma (Fig. 6).

A comparison of the detrital FTGA distribution (Fig. 6a) with the results of FT dating of apatite from bedrock exposures (Fig. 6b; filled points, fitted with exhumation rates; from Wagner *et al.* 1977, 1979) provides an instructive comparison. On the plot of bedrock FT ages (Fig. 6b), it should be noted that the upper slope is 410 m Ma^{-1} at an interval of about 14.2 Ma, and the lower slope shows exhumation of *c.* 260 m Ma^{-1} at about 11.7 Ma. Several important features appear in this comparison. First, we note that the young peak age, P1 (14.8 ± 1.2 Ma), is not significantly different from the average of the high-elevation bedrock samples (mean of 14.2 ± 0.7 Ma), which suggests that the bulk of the sediment of this detrital sample was derived from high elevations (*c.* > 1000 m). Second, the older peak age is not well represented in the bedrock data, which could indicate that rocks that cooled at *c.* 20 Ma are not well sampled in this area (presumably these high-elevation rocks are more difficult to reach). Although the peak widths in this sample are wide, they are well fitted to the data because of the high average uranium content and the large number of grains counted (n = 115). In this case, we can see that the detrital grain ages provides an excellent sample of the bedrock in the drainage system.

Erosion rates of the Indus River drainage basin, Pakistan

In this example, we look at an emerging technique of using each single zircon to estimate long-term erosion rates. We apply this approach to modern sediment dated by Cerverny *et al.* (1998) from the upper part of the Indus River drainage basin in Pakistan, which here extends from the foothills of the Himalaya to the southern margin of the Tibetan Plateau. Although this sort of analysis is under development by our group, it promises to provide a simplified approach to interpreting FTGA. Upstream from the sample collection point, the Indus River drains the Nanga Parbat–Haramosh massif with zircon FT ages of <3.2 Ma, as well as a variety of terranes with much older cooling ages (Zeitler 1985; Cerveny *et al.* 1988). The highest exhumation rates for the Nanga Parbat–Haramosh massif are estimated to be *c.* 5000 m Ma^{-1} but rates for surrounding areas are much lower (Zeitler 1985; Zeitler *et al.* 1993).

Our goal in this example is to estimate spatially averaged erosion rates over the entire drainage basin using a FTGA distribution. Modern erosion rates are commonly estimated from measurements of sediment yield, which is defined as the flux of sediment carried by a river, as normalized by the area of the upstream drainage system. The units used are volume of equivalent solid rock removed per time and area of the drainage system, with units of km Ma^{-1} (i.e. mm a^{-1}).

Lag time measures the amount of time needed

to erode the source terrane to a depth equal to the closure depth Z_c, which depends on the temperature profile during erosion and the closure properties for the thermochronometer being used. Here we make the assumption that the basal heat flux is relatively constant and that steady erosion is the primary factor controlling the shape of the temperature profile and the rate of cooling of the rocks. There are a few relatively young intrusions in the Nanga Parbat area (Zeitler *et al.* 1993), erosion rates may be slightly overestimated for this part of the drainage (i.e. zircon FT ages reflect cooling of magma, and not cooling induced by exhumation).

The steps in our analysis are illustrated and explained in Fig. 7a–d. Ceverny *et al.* (1988) dated two zircon mounts with different etch times; we mixed the results from the mounts in a manner designed to correct for grain-age bias (Garver & Brandon in preparation). This figure emphasizes some of the general aspects involved in transforming the FTGA probability density plot (Fig. 7a) to a plot of the erosion-rate distribution as a function of fractional and cumulative (Fig. 7c and d) drainage area. The transformation of the lag time to erosion rate is based on the relationships shown in Fig. 3.

An additional transformation is needed to account for the fact that erosion rate influences the volume of sediment and ultimately the relative proportion of the dated detrital mineral present in the FTGA distribution. To illustrate this point, let us consider a hypothetical drainage where half the basin is eroding at 500 m Ma^{-1} and the other half at 1000 m Ma^{-1}. The two source terranes yield zircon FT ages indicating lag times of 15 Ma and 5 Ma, respectively. The relative flux of sediment will be different by a factor of two because of the factor of two difference in erosion rate. Let us assume that the rocks in each source terrane have approximately the same density of datable zircons. If correct, then we would expect that a probability density plot constructed for a sample of zircon FT grain ages would have two peaks, with the young peak being twice the size of the old peak. This bias can be corrected by dividing the probability density by the associated erosion rate and then renormalizing the density to a probability mass of one. The peaks on this plot would have equal size, reflecting the fact that they each represent equal areas within the drainage system. Without this correction, the estimated average erosion rate would have a substantial upward bias.

Our findings suggest that the mean erosion rate for the Indus River (Fig. 7) is about 560 m Ma^{-1}, and a small part of the basin has erosion rates in excess of 1000 m Ma^{-1}. This result is surprising given that the drainage system is surrounded by the highest peaks in the world. We infer that high rates are only locally developed in the drainage.

Exhumation of the Coast Plutonic Complex, Western Canada

Perhaps the most complicated yet most promising of detrital FT techniques involves calculating interval exhumation rates based on mineral pairs from detrital apatite and zircon. In particular, if we were able to look at small differences in T_c, we could reduce the time interval over which our long-term exhumation rates are averaged. In this example, we look at how apatite and zircon peak ages can be compared to estimate exhumation rates.

The Tofino basin in southwestern British Columbia (BC) and northwest Washington State contains a nearly continuous sequence of Eocene to Miocene marine strata derived from the Coast Mountains of British Columbia in western North America (Fig. 8). In a recent study of detrital zircon from strata of this basin, Garver & Brandon (1994*b*) showed that quartzofeldspathic sandstones from this basin record the erosional unroofing of the Coast Plutonic Complex (CPC) and related rocks in the Coast Range Mountains. The zircon fission-track record revealed that component populations became successively younger upsection, indicating progressive unroofing of a metaplutonic source terrane. This progressive unroofing and exhumation produces a well-developed forward moving peak. From these data, Garver & Brandon calculated constant long-term (30–40 Ma) exhumation rates of about 250 m Ma^{-1} throughout much of Tertiary time, which suggests that the erosional system was in a steady state.

Here, we supplement this analysis by presenting apatite fission-track ages for some of the samples reported by Garver & Brandon (1994*b*) (a full set of data is available as SUP 18128, see p. 290). Then, we estimate exhumation rates using mineral pairs (apatite–surface and apatite–zircon). These model exhumation rates are used.

Strata of the Tofino basin are mostly offshore, but they are locally exposed as a tilted sequence of Eocene and younger marine sedimentary rocks on the Olympic Peninsula of Washington State (Tabor & Cady 1978; Muller *et al.* 1983; Brandon & Vance 1992; Garver & Brandon 1994*b*). The BC Coast Mountains are dominated by the CPC, which is composed of Jurassic to Tertiary quartz diorites to granodiorites that

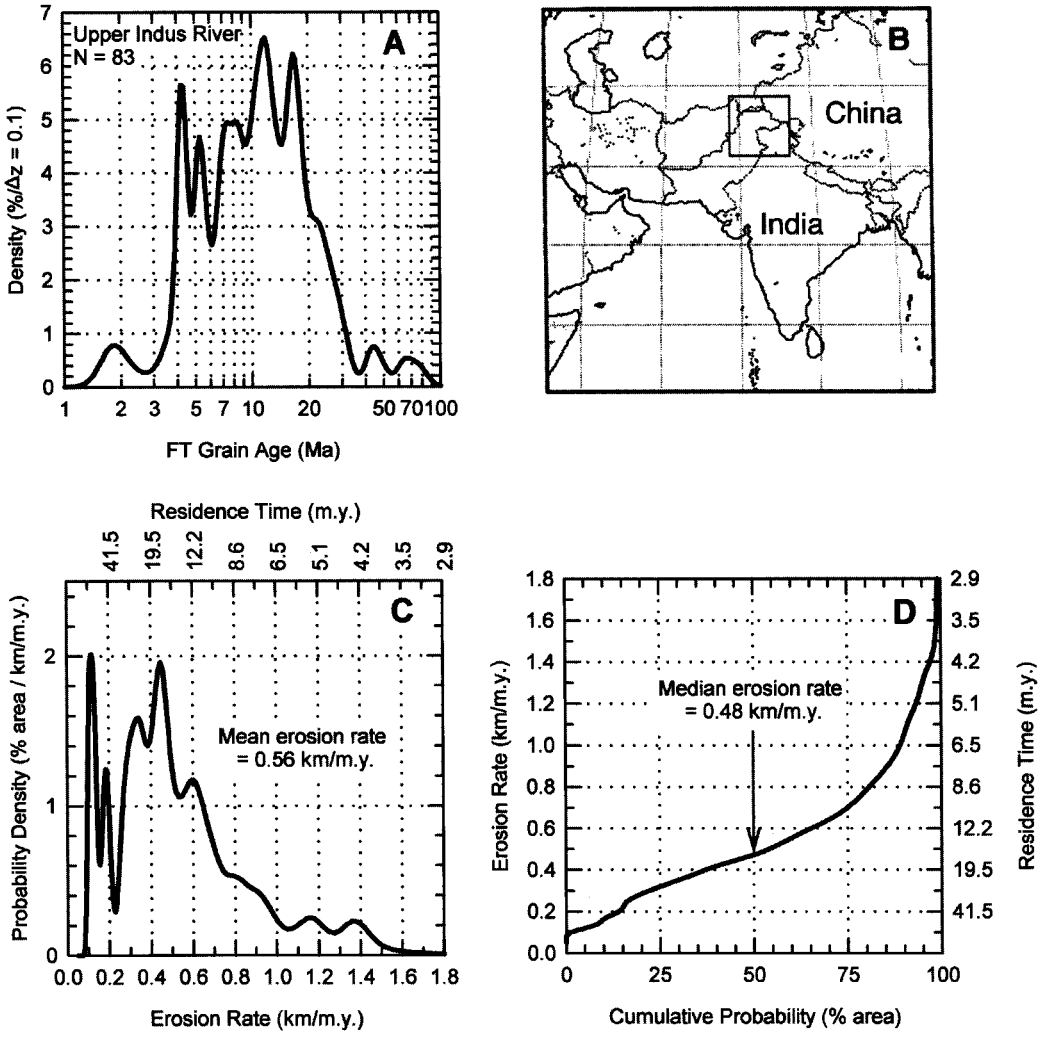

Fig. 7. Transformation of a detrital FTGA distribution to an erosion-rate distribution using data from the Indus River in Pakistan (data from Cerveny *et al.* 1988). (**a**) The FTGA distribution for detrital zircons from modern sands of the Indus River in Pakistan, as reported by Cerveny *et al.* (1988). The PD plot was constructed using the method of Brandon (1996). Probability density is given in number of grains per *c.* 10% increments on the grain-age scale. (**b**) Location map for sample. (**c**) The PD plot for erosion rate was converted from the FTGA PD plot using the erosion rate–lag time relationship for zircon FT ages present in Fig. 3. Probability density was normalized to relative area by scaling the transformed PD relative to the inverse of the erosion rate. The mean erosion rate is *c.* 560 m Ma^{-1}. (**d**) The cumulative probability of erosion rate by area was calculated by integrating the PD plot in (**c**). The median value (50%) is *c.* 480 m Ma^{-1}. This plot indicates that *c.* 10% of the basin has erosion rates faster than 1000 m Ma^{-1}.

extend nearly 1500 km from southernmost BC north to Alaska (Roddick 1983). Significant uplift and exhumation of the BC Coast Mountains, particularly pronounced and well documented in the north–central section, is known to have occurred after intense Paleocene–Eocene plutonic and orogenic activity (Fig. 8; Parrish 1983). Following this activity, rapid cooling and exhumation of the central and northern BC Coast Mountains occurred at *c.* 55 Ma (Cook & Crawford 1996) with exhumation rates that may have been as high as *c.* 2000 m Ma^{-1} (Hollister

1982). Following this event, the north-central part of the BC Coast Mountains had apparent exhumation rates of *c.*150 m Ma^{-1} from 25 to 15 Ma (Parrish 1983), but about 250–300 m Ma^{-1} at 35–45 Ma and about 400 m Ma^{-1} at 30–40 Ma. These studies indicate that sediment shed from this north–central source should have a distinct thermal history marked by rapid and widespread cooling at *c.*55 Ma and relatively slow cooling after this event.

We now consider the sedimentary record of this exhumation history (Figs 9 and 10; Tables 2–4). First, we correlate the main peak in each distribution based on the assumption that the main peak contains the majority of the grains, that it becomes younger with time, and that

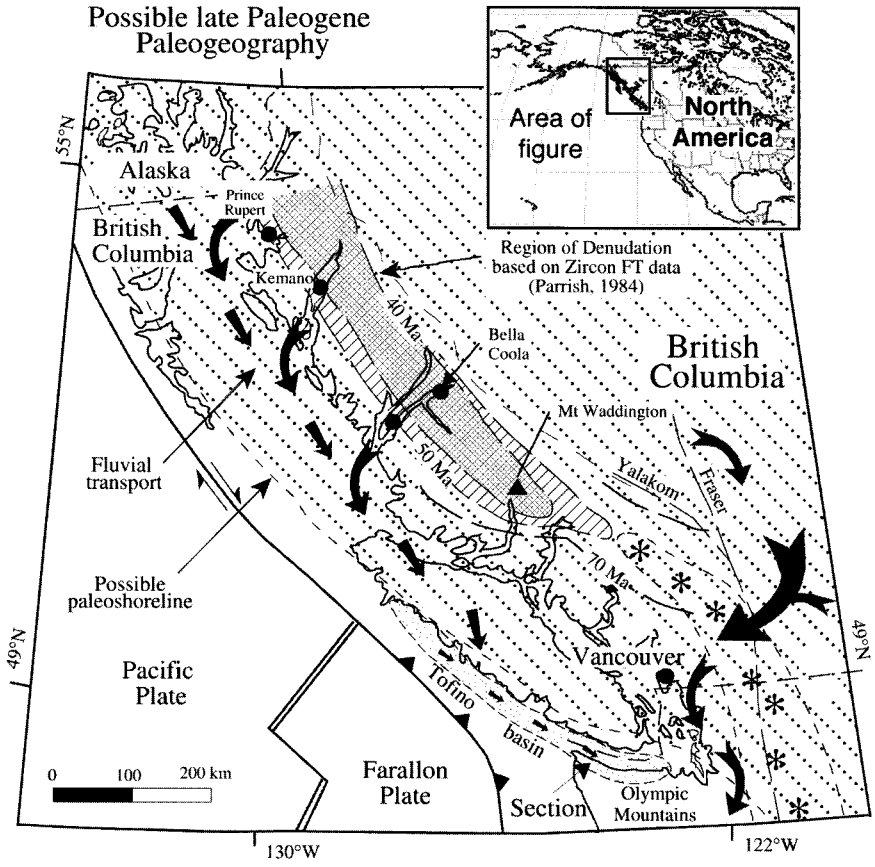

Fig. 8. Location map and inferred Paleogene palaeogeography of the Coast Plutonic Complex in western British Columbia, Canada. In this setting, two important sediment sources are identified. The first is sediment derived from the Cascade arc (shown schematically by '*') and a variety of thermotectonic source terranes in the back-arc region. The back-arc sediments mix with sediments from the arc, and ultimately are transported to the forearc. The second is sediment derived from the progressive uplifted and exhumation of the BC Coast Mountains, dominated by dioritic rocks of the Coast Plutonic Complex, which is the focus of our third example. Although most of this sediment from the BC Coast Ranges was shed westward, much of it flowed south along the continental margin and was ultimately deposited in the Tofino basin, which extends as far south as northern Washington State. In the BC Coast Ranges, FT data from bedrock give an important baseline cooling history with which we compare our results (see Parrish 1983). The occurrence of Coast Plutonic Complex-derived sediments in the Tofino basin suggests that the area was largely emergent and fluvial transport was responsible for much of the sediment movement (arrows) to the south. The stratigraphic section from which our samples were derived is labelled 'section', which occurs along the northern edge of the Olympic Mountains in the USA (Washington State).

apatite peaks are younger than the zircon peaks for a particular source. Using this approach, we can compare the main peak in the three uppermost samples (Table 3, Fig. 10). That the lag between the dominant apatite peak age and the dominant zircon peak age becomes smaller with time and is very close in age to the youngest unit examined (Clallam), indicates rapid exhumation at this time (here *c.* 56 Ma). Next, the peak lag and exhumation rate for these peaks can be calculated for all the peaks (Table 4). The peak lag is the difference between the peak ages (i.e. for apatite and zircon) or the difference between the peak age and deposition. Both estimates give us an indication how long it took for the source rock to move between one datum and the next (Table 4).

Calculated exhumation rates range between about 100 and 1500 m Ma^{-1} for the main peak. This peak is attributed to unroofing of the Coast Plutonic Complex, which has estimated exhumation rates of *c.* 120 and 230 m Ma^{-1} during the interval between *c.* 34 and 54 Ma (Parrish 1983). The zircon–apatite peaks in the Clallam Formation suggest exhumation rates of about 1500 m Ma^{-1} at *c.* 56 Ma. This result is consistent with other studies that suggest rapid cooling occurred at about this time, or slightly younger, with exhumation rates as high as *c.* 2000m Ma^{-1} (Hollister 1982; Cook & Crawford 1996).

The preceding discussion demonstrates several important aspects of using apatite and zircon FT chronology together. Because peak widths vary according to age and uranium concentration, apatite peaks are almost always more poorly resolved than zircon peaks. Our experience suggests that this difference in precision makes comparisons between apatite and zircon FT ages possible only if (a) apatite statistics are improved by counting a large number of grains (100 or more) present in the distribution, (b) there are only a few peaks (one to two), and (c) peaks are well separated in time (by more than 20–30% of their peak ages).

Exhumation of Fiordland, South Island, New Zealand

Rocks of Fiordland in New Zealand consist of a Palaeozoic to Mesozoic metaplutonic complex that has experienced episodic exhumation since Cretaceous time, which is well recorded in the flanking strata of the Te Anau basin (Figs 11 and 12). In this example, we show how fission-track ages of detrital apatite samples record the exhumation of Fiordland during the establishment of the modern plate regime which is dominated by the Alpine Fault, a major oblique-slip fault that separates the Pacific and Australian plates. This example illustrates how strata from the perimeter of a basin can be used to avoid problems with thermal resetting, which would be expected for detrital apatite in a central more deeply buried part of the basin (Fig. 1). In the case of the Te Anau basin, most of the basin fill has been buried deeply enough to have thermally affected apatite, and most of the provenance information has been lost because of thermal resetting.

The Te Anau basin has been a long-lived depocentre from Eocene to Recent time, and as a result it has received some 8000 m of sediments from adjacent terranes (Turnbull *et al.* 1993). The Fiordland block, in which plutonic and metaplutonic rocks form the basement to the western edge of the basin, has been a major contributor of detritus to the basin. One of the main source regions for sediment in the Te Anau basin was the Fiordland block. In Late Eocene time, subsidence rates accelerated, but in Early Oligocene time, the basin received a thick sequence of marine sediments derived from Fiordland (Turnbull *et al.* 1993). It is widely thought that the Eocene to Oligocene phase of sedimentation was driven by a new transtensional regime set up during plate reorganization at this time (e.g. Stock & Molnar 1982). Here and elsewhere in New Zealand, Middle to Upper Oligocene strata are dominated by carbonate rocks, which suggests a period of tectonic quiescence. Lower to Middle Miocene sediments of the Te Anau basin record deep-marine conditions in the centre of the basin but shallow marine facies along its western margin. Although much of the detritus in this interval is mudstone, some units on the western margin, including the Borland Formation (Fig. 12), are coarse grained and derived from Fiordland (Turnbull *et al.* 1993). In late Mid-Miocene to Pliocene time, the Prospect Formation records an enormous increase in sediment derived from adjacent terranes. Palaeocurrents and pebble types suggest that for the Prospect Formation, palaeoflow was generally to the south. The source region included terranes to the northeast (Caples), but also Fiordland rocks (Turnbull *et al.* 1993). This final phase of sedimentation is related to contraction and uplift along the Alpine strike-slip fault system.

An important aspect of our analysis here, and the reason that we selected samples along the basin periphery, is that although the total fill of the Te Anau basin is thick in the centre of the basin, successive phases of uplift have resulted in onlap of the strata onto the edge of the

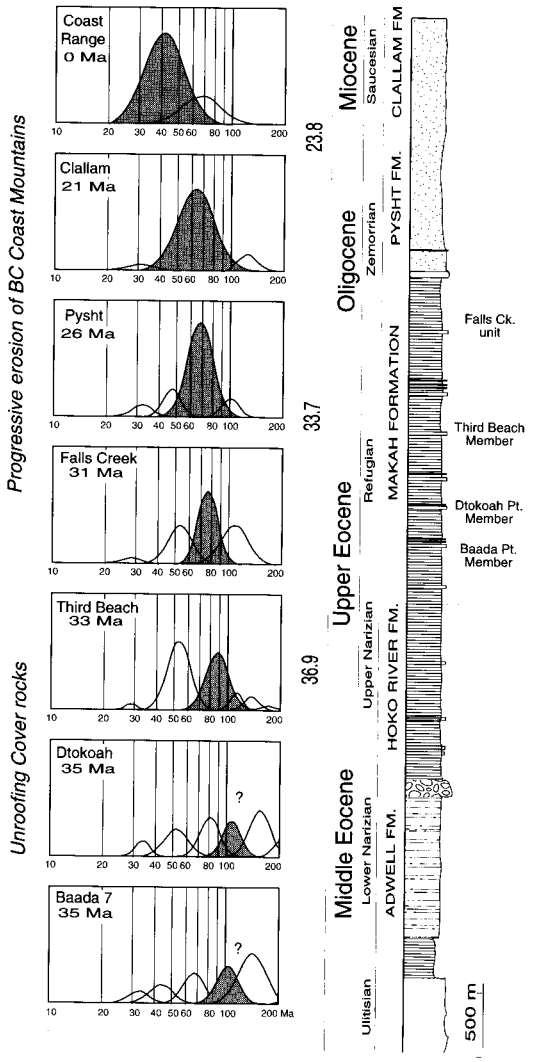

Fig. 9. Stratigraphy of part of the Tofino basin (in Washington State, USA) showing the forward moving peaks of FT grain ages of detrital zircon (modified from Garver & Brandon 1994*b*). It should be noted that the uppermost plot shows all data from the northern Coast Plutonic Complex (bedrock, from Parrish 1983), treated as if all dated grains were detrital (see Garver & Brandon 1994*b*). A comparison of apatite and zircon peak ages for the upper three units is shown in Fig. 10.

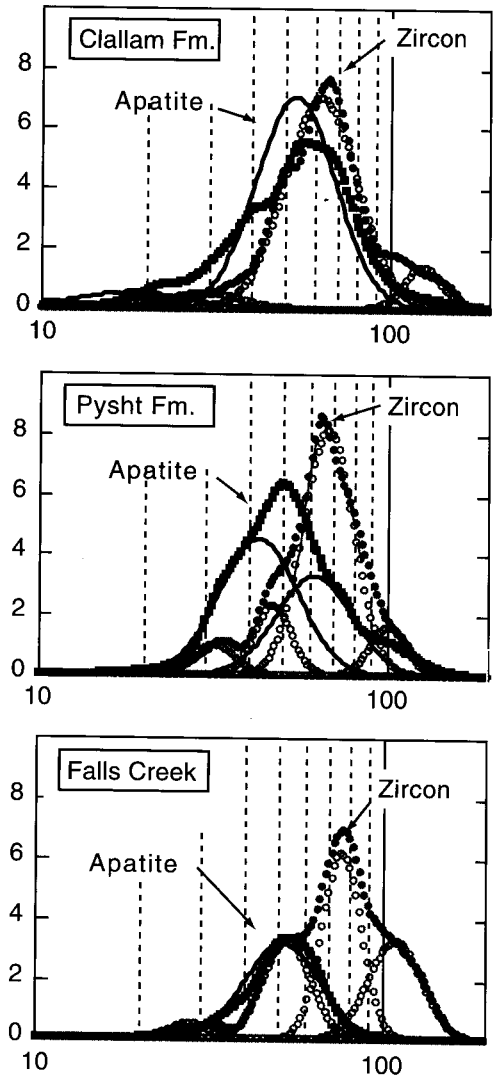

Fig. 10. Comparison of zircon and apatite peak ages from the three upper units of the Tofino basin exposed on the northern flanks of the Olympic Peninsula in Washington State (USA). Samples shown from oldest at the bottom to youngest at the top. Sediments in these units are inferred to have been derived from the Coast Plutonic Complex. The FT ages record the progressive erosion of this area through time (Garver & Brandon 1994*b*). Shown are the PD plot for zircon (○) and apatite (■) along with the fitted peak ages for zircon (●) and apatite (continuous lines). It should be noted that the difference in the main peak age between apatite and zircon becomes shorter with time, which is inferred to represent the exhumation of a rapidly cooled section of upper crust at *c.* 56 Ma.

Table 2. *Comparison of zircon and apatite FT peak ages from detritus shed from the BC Coast Ranges, Canada*

Mineral	Age range (Ma)	P1	P2	P3	P4	P5
Clallam Formation (depositional age is 17.7–24.1 Ma)						
Zircon (N_t = 51)	19–147	22.5 ± 1.9 (4%) W = 0.25	58.9 ± 4.7 (68%) W = 0.25	77.3 ± 6.8 (15%) W = 0.25	117.8 ± 9.3 (26%) W = 0.25	–
Apatite (N_t = 50)	08–127	18.1 ± 3.4 (8%) W = 0.33	53.3 ± 2.5 (92%) W = 0.26	–	–	–
Pysht Formation (depositional age is 24.1–28.5 Ma)						
Zircon (N_t = 50)	29–110	37.3 ± 2.8 (9%) W = 0.22	63.8 ± 4.6 (74%) W = 0.22	92.9 ± 6.8 (18%) W = 0.22	–	–
Apatite (N_t = 50)	25–109	–	42.9 ± 4.9 (59%) W = 0.26	62.1 ± 10.9 (41%) W = 0.25	–	–
Falls Creek Unit (depositional age is 28.5–32.7 Ma)						
Zircon (N_t = 50)	26–136	28.7 ± 2.1 (4%) W = 0.21	50.5 ± 3.6 (17%) W = 0.21	72.1 ± 5.2 (46%) W = 0.21	103.4 ± 7.4 (27%) W = 0.21	135.4 ± 9.9 (6%)
Apatite (N_t = 20)	18–110	–	–	51.5 ± 2.9 (100%) W = 0.25	–	–

For zircon (see Garver & Brandon 1994*b*), fractions were hand picked, and then two equal portions were mounted in FEP Teflon, polished, and etched in a KOH–NaOH eutectic at 225°C for 12–20 h; one mount was given a 'long' etch, and the other was given a 'short' etch (see Naeser *et al.*, 1987). The etched mounts were irradiated at the Oregon State nuclear reactor using a nominal fluence of 2×10^{15} neutrons cm^{-2}. The internal gradient within the irradiated package was estimated by interpolating track densities for fluence monitors (CN-5) placed within of the irradiation tube. Fission tracks were counted at 1250× (100× oil immersion objective, 1.0 tube factor, 12.5× oculars) on an Olympus BH-2 microscope. Ages were calculated using an mean weighted $zeta_{CN\text{-}5}$ of 323.5 ± 9 (±1 SE; J.I.G. at Union). Apatite grains were mounted in epoxy resin on glass slides and polished to expose internal grain surfaces. The mounts were then etched in 5 M HNO_3 for 20 s at 21°C. Samples were irradiated at the Oregon State nuclear reactor with a nominal fluence of 5×10^{15} neutrons cm^{-2}. Samples were irradiated with the glass dosimeter CN-1 as well and the Fish Canyon Tuff, Durango and Mt Dromedary apatite age standards. Apatite grains were counted using a Leitz Ortholux microscope at 1600× (160× dry objective and 10× oculars). Ages were calculated using a $zeta_{CN\text{-}1}$ of 105.8 ± 2.5 (±1 SE; M.R.-T). FT data were decomposed using a peak-fitting routine of Brandon (1992). In this routine, grain ages are calculated, the grains are ordered in increasing age and the resultant distribution of grain ages is fitted with a probability density distribution. The probability distribution invariably represents several component populations, which must be extracted using a peak-fitting routine, which fits individual peaks to the probability density plot. For zircon we use the Gaussian peak-fitting routine of Brandon (1992), and for apatite we use the binomial fitting routine of Galbraith & Green (1990).

Table 3. *Summary of principle detrital peaks used in model calculations, detritus from the BC Coast Ranges, Canada*

		Peak 1	
Clallam	Z	58.9	(68)
	A	53.3	(92)
	S	21.0	
Pysht	Z	63.8	(74)
	A	42.9	(49)
	S	26.0	
Falls Ck	Z	72.1	(46)
	A	51.5	(100)
	S	31.0	

Z, Zircon; A, apatite; S, surface or depositional age. Numbers in parentheses are the percentage of grains that make up the peak.

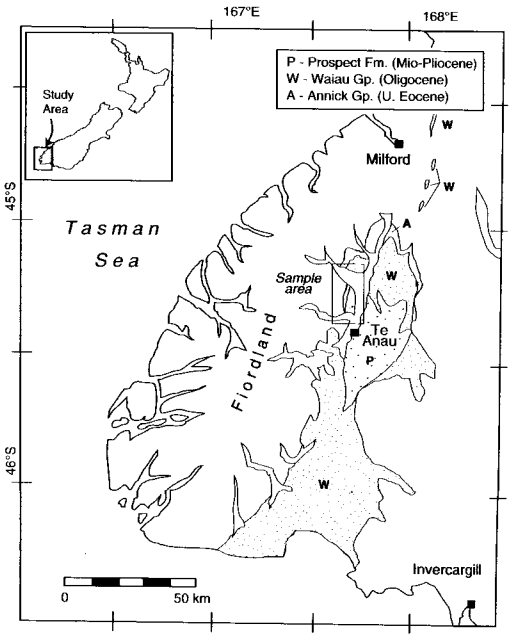

Fig. 11. Simplified geological map of the Fiordland area in the southern part of the South Island, New Zealand, showing basement rocks and adjacent basin strata of the Te Anau basin. P, Prospect Formation; W, Waiau Group throughout most of the basin but also includes the Nightcaps Group along the SE edge of the exposed basin; A, Annick Group; B, basement terranes including only locally minor exposures of Eocene to Cretaceous strata (southern tip of Fiordland; see Fig. 12 for ages and stratigraphy). (Modified from Turnbull *et al.* 1993.)

Fiordland block. The result is that basin-margin strata are relatively condensed in thickness. Thus the section there preserves a long record without the complication of thermal annealing of the apatites.

Density plots with fitted peaks are shown for samples with depositional ages spanning some 15 Ma from *c.* 34 to 20 Ma (Fig. 12; Table 5). This suite of samples records a 15 Ma interval that includes initial rifting, subsequent waning of tectonic activity, and finally the establishment of the Alpine Fault system at *c.* 23 Ma. The data have several important features and the results can be evaluated into two groups; a group deposited between *c.* 35 and 32 Ma and one deposited between *c.* 29 and 20 Ma. The older samples contain two peaks (P1 and P2) that become older with time (Fig. 13). This is an unusual situation because generally FT peak ages move forward as a source is exhumed with time. Progressively older component ages in

Table 4. *Model exhumation rates based on comparing main peak age in apatite and zircon from detritus from the BC Coast Ranges, Canada*

Unit	Age (or t_d) (Ma)	Pair	Lag time (Ma)	Midpoint (Ma)	Z (km)	$\dot{\varepsilon}_{model}$ (m Ma^{-1})
Pysht	26	AS	16.8	34.5	4.5	266
Clallam	21	AS	32.3	37.5	4.5	140
Falls Creek	31	AS	20.5	41.3	4.5	220
Pysht	26	ZA	20.9	53.4	4.9	234
Clallam	21	ZA	2.8	56.1	4.9	1600
Falls Creek	31	ZA	20.6	61.8	4.9	238

Pair refers to the thermochronometers used (ZA, zircon–apatite pair; AS, apatite–surface pair). Lag time is the peak lag (PL_1 Ma) (peak age – depositional age) for samples going to the surface; peak age minus peak age for mineral pairs) for individual samples. This number represents the time it took rock to pass from one known isotherm to either the surface or another known isotherm. Midpoint ages represent the time between closure of each system, and the table is sorted on midpoint ages because these show model erosion rates through time. Depth is the crustal thickness based on model assumptions as outlined in text. $\dot{\varepsilon}_{model}$ represents the model rate calculated for the interval; based on a generic geotherm of 25°C km^{-1} as outlined in text.

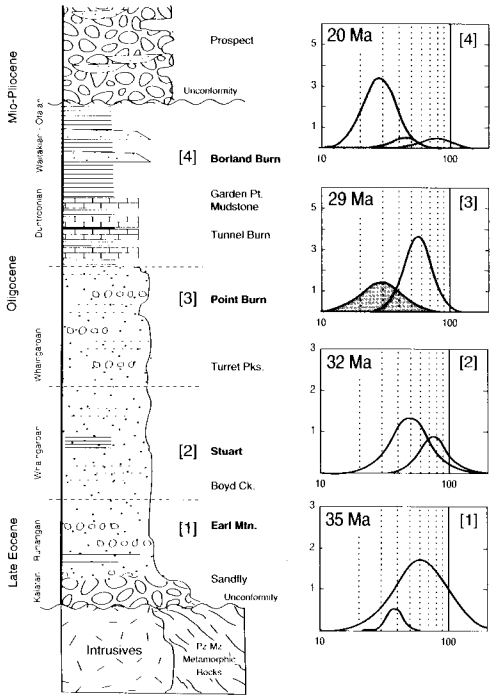

Fig 12. Stratigraphy and FT peak ages for detrital apatite from strata on the flanks of the Fiordland block in the southern part of the South Island, New Zealand (see Table 5). In this upsection progression, we recognize two suites of samples. The first suite (35 and 32 Ma) is inferred to represent the initial unroofing of cover strata, and it is possible that this group has backward-moving peaks as explained in the text. The second suite (29–20 Ma) shows the emergence and then dominance of a young peak that we infer to be associated with exposure of reset rocks that resided below the partial annealing zone before exhumation. This young peak (P1, shaded, in both the 29 and 20 Ma samples) does not become significantly younger with time, which suggests that rapid exhumation occurred at *c.* 30 Ma (>5000 m Ma^{-1}) followed by slow exhumation between 29 and 20 Ma (*c.* <500 m Ma^{-1}). Stratigraphy is a schematic representation derived from data and descriptions of Turnbull (1985), and Turnbull *et al.* (1993).

younger and younger strata, referred to as a backward moving peak, may represent the downward removal of cover strata that have an unroofing sequence preserved in their layers.

The younger two samples record very rapid exhumation of Fiordland rocks at about 30 Ma, followed by slow and continuous erosion. In these two younger samples, the young (P1) age is about the same (*c.* 29 Ma) despite the fact that the these samples were deposited about 9 Ma apart. The occurrence of a peak age in strata that have essentially the same age (lag time *c.* 1 Ma or less; see Table 5) suggests that exhumation rates were extremely rapid at this time (*c.* 29 Ma), probably in excess of 2000 m Ma^{-1} (Fig. 3). In the youngest strata, the peak age remains about the same (*c.* 29 Ma) and the peak lag is about 7 Ma. In this case, exhumation of the source terrane must have slowed abruptly to below 500 m Ma^{-1} as this would be the average rate over this interval (between 29 and 20 Ma); otherwise, if exhumation was progressive through this time, the peak age would have progressively younged with time (a typical 'moving peak'). In previous work, we have referred to this as a static peak and have interpreted the peak age to represent the time of rapid crustal quenching (Brandon & Vance 1992; Garver & Brandon 1994*a*,*b*). This pattern is the hallmark of extensional exhumation where a substantial thickness of crustal section is rapidly cooled because of normal faulting.

The reduction in exhumation rates of P1 is supported by the fact that during this interval (*c.* 27–23 Ma; Late Oligocene) most of New Zealand was covered by shallow-marine limestones. Only after initiation of the Alpine Fault (*c.* 23 Ma) did rocks retaining this 'static peak' become uplifted, deeply eroded, and shed into adjacent basins. The onset of motion on the Alpine Fault is marked by widespread clastic sedimentation in New Zealand. Therefore, the erosion of rocks with this cooling age appears to have been episodic. For example, at *c.* 20 Ma, the lag time for P1 is about 7 Ma, giving an average exhumation rate over this entire interval of about 500 m Ma^{-1}. None the less it seems likely that the instantaneous exhumation rate during this interval could have been much greater (> 1000 m Ma^{-1}) sometime during this 7 Ma interval. Based on what we know about the tectonic history of New Zealand, rapid exhumation was likely at the *c.* 29 Ma because of rifting and at *c.* 23–20 Ma because of inception of the Alpine Fault.

In this example, we have shown several important aspects of using detrital apatite to understanding exhumation. First, it is important to sample rocks that have not been thermally annealed. In this regard, condensed sections around the perimeter of a basin are very attractive candidates. Second, peak ages with short lag times indicate rapid exhumation. Third, erosion of 'cover rocks' or the 'dead zone' must precede exhumation of deeply buried rocks (sub-PAZ). The dead zone does not contain a thermal signal of the exhumation event and several possibilities

Table 5. *Apatite FT peak ages for the Te Anau basin, Fiordland, New Zealand*

Unit	NZ stage	Age (Ma)	Range (Ma)	*n*	P1	P2	P3	Track length	SD	(*n*)
Waiau Gp	Otaian	*c.* 20.5	(18.7–22.0)	32	28.5 ± 1.7 *W*= 0.30 79%	45.7 ± 8.4 *W* = 0.28 11%	77.8 ± 12.4 *W* = 0.28 10%	13.36 ± 0.58 13.20 ± 0.28	1.15 1.41	(05) (61)
Waiau Gp	Upper Whaingaroan	*c.* 29.0	(28.0–30.0)	36	29.4 ± 3.2 *W* = 0.37 37%	56.4 ± 3.2 *W* = 0.25 63%	–	11.54 ± 0.40 11.43 ± 0.28	2.18 2.18	(29) (60)
Waiau Gp	Lower Whaingaroan	*c.* 32.0	(30.0–34.0)	17	49.1 ± 5.2 *W*= 0.35 68%	75.9 ± 5.2 *W* = 0.25 32%	–	11.40 ± 0.54 11.49 ± 0.47	1.85 1.15	(29) (07)
Annick Gp	Runangan	35.0	(34.0–36.0)	22	38.1 ± 2.8 *W* = 0.14 8%	61.9 ± 2.7 *W* = 0.47 91%	–	11.95 ± 0.27	1.76	(42)

Apatite grains were mounted in epoxy resin on glass slides and polished to expose internal grain surfaces. The mounts were then etched in 5 M HNO_3 for 20 s at room temperature. With low-uranium mica flakes affixed to the polished and etched mounts, the samples were irradiated at the X-7 facility of the HIFAR reactor, Lucas Heights, Australia, (following procedures outlined by Kamp *et al.* (1992)) with a nominal fluence of 10×10^{15} neutrons cm^{-2}. Samples were irradiated with the glass dosimeter SRM 612 as well, and the Fish Canyon Tuff, Durango and Mt Dromedary age standards. Grains were counted using a Leitz Ortholux microscope at 1250× (100× dry objective, 1.25 tube factor, and 10× oculars). Ages were calculated using a mean weighted $zeta_{SRM612}$ of 348.7 ± 4.3 (±1 SE; I.W.S.W.) or 343.5 ± 4.5 (±1 SE; I.J.L.). Data from two separate samples were combined for each analysis, and track lengths are shown for each sample, with the exception of one sample of the Annick Group in which no lengths were measured. Peak ages calculated using a binomial statistical analysis, with the exception of the oldest sample, which was fitted using a Gaussian approximation because it is poorly approximated by binomial statistics (for procedure and program see Brandon (1996)). Depositional age approximated from regional stratigraphy. *W* is the fraction of the half-width of the peak. The percentage of grains that compose each peak are shown below *W*. The number of grains in each analysis is represented by *n*.

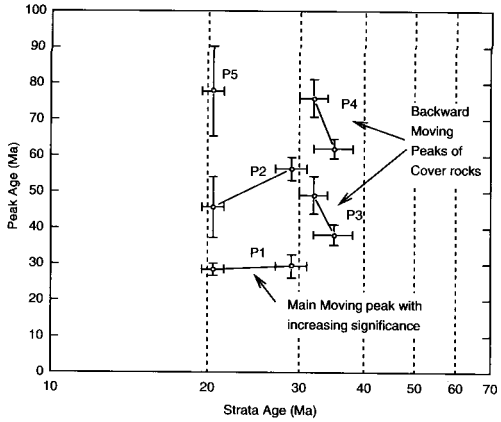

Fig. 13. Relationship between peak age and strata age for apatite FT ages of the Te Anau basin, Fiordland, New Zealand. It should be noted that the older strata contain older peak ages inferred to have been derived from reworking of sedimentary rocks. The younger peaks, especially P1, are inferred to represent the exhumation of plutonic rocks of Fiordland.

exist as the detrital FT pattern that may result from erosion of this crustal layer. In some cases, older PAZs fossilized in previous exhumation events may give younger and younger peak ages as erosion uncovers deeper levels. This situation results in forward moving peaks, which track successive incision into the dead zone. In other cases, the dead zone may consist of basin strata that have not been thermally annealed. In this case, the resulting pattern of FT grain ages can be complicated because of recycling of older unreset detritus. It is possible that in the case of exhumation of basin strata, backward moving peaks may result from erosion of cover strata that have a pre-existing unroofing signature (Garver & Brandon 1994*b*).

Conclusions and future directions

These studies highlight the advantages and approach of detrital FTGA analysis. A few general observations can be made about application of this approach to understanding exhumation. First, the evolution of exhumation is best evaluated when samples are collected from a well-dated stratigraphic section that spans the exhumation event. Second, a condensed section from the perimeter of a basin is most likely to preserve unreset detrital grains and therefore give provenance information. This problem is especially acute for apatite. Third, during erosion, the removal of cover rocks or a 'dead zone' precedes the exposure of rocks with young cooling ages. Fourth, fast exhumation results in short lag times and slow exhumation results in a long lag time. Steady-state conditions are reflected in a constant lag time. Fifth, for most source regions with several distinct cooling ages, about 50 grain FT grain ages will capture the principle grain-age populations, but more grain ages will give better resolution. In cases where zircon and apatite ages from the same sample are compared, the comparison is easiest when samples have high-uranium apatite grains (>50 ppm), and numerous apatite grains have been counted (>100).

A variety of studies are required to advance detrital FT thermochronology. To quantitatively evaluate FT ages of different mineral systems, future work needs to address the relative proportion of apatite and zircon grains derived from various source rock lithologies, as well as the fate of these minerals in transport, burial, and diagenesis. In particular, there is a need to obtain a full quantitative sampling of FT grain ages free from procedural biases. Although probably small, there are several important aspects of etching and counting that need to be evaluated in this context. Finally, a better understanding of the thermal history of individual grains and effective closure temperature of each individual grain will also advance this approach. This avenue of research involves understanding the annealing characteristics of individual grains through crystal-specific constraints based on chemistry, track lengths, or etch pit size in apatite. In zircon,there is a need to resolve the effective closure temperature of zircon as well as the relationship between alpha damage and closure temperature.

This work was funded directly and indirectly by National Science Foundation grant EAR 9614730 and EAR 9418989 (to J.I.G.), EAR 9005777 and EAR 9418989 to M.T.B., and EAR 9117941 to M.R.-T. Irradiation was funded, in part, by the Reactor Use Sharing (R.U.S.) programme awarded to B. Dodd and the Oregon State Reactor Facility. M. E. Bullen collected and separated the sample from the Italian Alps. J.I.G. gratefully acknowledges logistical support of the Department of Earth Sciences at the University of Waikato, New Zealand, during a 1997 sabbatical leave. This paper benefited from helpful review by G. Lister and three anonymous reviewers.

References

BALDWIN, S. L., HARRISON, T. M. & BURKE, K. 1986. Fission-track evidence for the source of accreted sandstones, Barbados. *Tectonics*, 5, 457–468.

BRANDON, M. T. 1992. Decomposition of fission-track grain age distributions. *American Journal of Science*, **292**, 535–564.

—— 1996. Probability density plot for fission-track grain-age samples. *Radiation Measurements*, **26**, 663–676.

—— & VANCE, J. A. 1992. New statistical methods for analysis of fission-track grain-age distributions with applications to detrital zircon ages from the Olympic subduction complex, western Washington State. *American Journal of Science*, **292**, 565–636.

——, RODEN-TICE, M. K., & GARVER, J. I. 1998. Late Cenozoic exhumation of the Cascadia accretionary wedge in the Olympic Mountains, northwest Washington State. *Geological Society of America Bulletin*, **110**, 985–1009.

BROWN, R., SUMMERFIELD, M. A. & GLEADOW, A. J. W. 1994. Apatite fission-track analysis: its potential for the estimation of exhumation rates and implications for models of long-term landscape development. *In*: KIRKBY, M. J. (ed.) *Process Models and Theoretical Geomorphology*. Wiley, New York, 23–53.

CARTER, A. 1996. The application of FT provenance studies to paleogeographic reconstructions: an example from Thailand (abstract). *In*: *Abstracts for the International Workshop on Fission-track dating, Gent 1996*. Geological Institute and Institute for Nuclear Sciences of the University of Gent, 19.

CERVENY, P. F. 1988. *Uplift and erosion of the Himalaya over the past 18 million years: evidence from fission track dating of detrital zircons and heavy mineral analysis*. MS thesis, Dartmouth College, Hanover, NH.

——, NAESER, N. D., ZEITLER, P. K., NAESER, C. W. & JOHNSON, C. W. 1988. History of uplift and relief of the Himalaya during the past 18 million years: evidence from fission-track ages of detrital zircons from sandstones of the Siwalik Group. In: KLEINSPEHN, K. & PAOLA, C. (eds) *New Perspectives in Basin Analysis*, Springer, New York, 43–61.

CLARK, S. P., JR & JÄGER, E. 1969. Exhumation rates in the Alps from geochronologic and heat flow data. *American Journal of Science*, **267**, 1143–1160.

COHEN, H. A., ONSTOTT, T. C., LUNDBERG, N. & HALL, C. M. 1990. 40/39 Ar laser probe dating of detrital phenocrysts to constrain the age of volcanism, Gravina Belt, SE Alaska. *EOS Transactions, American Geophysical Union*, **71**, 1617.

COOK, R. D. & CRAWFORD, M. L. 1996. Exhumation and tilting of the western metamorphic belt of the Coast Orogen in southern southeastern Alaska. *Tectonics*.

COPELAND, P. & HARRISON, T. M. 1990. Episodic rapid uplift in the Himalaya revealed by $^{40}Ar/^{39}Ar$ analysis of detrital K-feldspar and muscovite, Bengal Fan. *Geology*, **18**, 354–357.

——, —— & HEIZLER, M. T. 1990. $^{40}Ar/^{39}Ar$ single-crystal dating of detrital muscovite and K-feldspar from Leg 116, southern Bengal Fan: implications for the uplift and erosion of the Himalayas. *In*: COCHRAN, J. R. & STOW, D. A. V. (eds) *Proceedings of the Ocean Drilling Program, Scientific Results*, **116**, Ocean Drilling Program, College Station, TX, 93–114.

CORRIGAN, J. D. & CROWLEY, K. D. 1990. Fission-track analysis of detrital apatites from sites 717 and 718, Leg 116, Central Indian Ocean. *In*: COCHRAN, J. R. & STOW, D. A. V. (eds.) *Proceedings of the Ocean Drilling Program, Scientific Results*, **116**, 75–87.

DALLMEYER, R. D., KEPPIE, J. D. & NANCE, R. D. 1997. $^{40}Ar/^{39}Ar$ ages of detrital muscovite within Lower Cambrian and Carboniferous clastic sequences in northern Nova Scotia and southern New Brunswick: applications for provenance regions. *Canadian Journal of Earth Sciences*, **34**, 156–168.

DILL, H.-G. 1994. Can REE patterns and U-Th variations be used as a tool determine the origin of apatite in clastic rocks? *Sedimentary Geology*, **92**, 175–196.

DODSON, M. E. 1979, Theory of cooling ages. *In*: JAEGER, E. & HUNZIKER, J. C. (eds) *Lectures in Isotope Geology*. Springer, Berlin, 194–202.

DUNKL, I., FRISCH, W., KUHLEMANN, J. & BRÜGEL, A. 1996. 'Combined pebble dating': a new tool for provenance analysis and for estimating alpine exhumation (abstract). *In*: *Abstracts for the International Workshop on Fission-track Dating, Gent 1996*. Geological Institute and Institute for Nuclear Sciences of the University of Gent, 32.

FLEISCHER, R. L., PRICE, P. B. & WALKER, R. M. 1975. *Nuclear Tracks in Solids*. University of California Press, Berkeley, CA.

FRISBEE, A. J. 1995. *A fission-track study of detrital zircons from Pacific Northwest river sediments*. BSc thesis, Union College, Schenectady, NY.

GALBRAITH, R. F. 1988. Graphical display of estimates having differing standard errors. *Technometrics*, **30**, 271–281.

—— & GREEN, P. F. 1990. Estimating the component ages in a finite mixture. *Nuclear Tracks and Radiation Measurements*, **17**, 197–206.

GARVER, J. I. 1988. Stratigraphy and tectonic significance of the clastic cover to the Fidalgo Ophiolite, San Juan Islands, Washington. *Canadian Journal of Earth Sciences*, **25**, 417–423.

—— & BRANDON, M. T. 1994*a*. Fission-track ages of detrital zircon from mid-Cretaceous sediments of the Methow–Tyaughton basin, southern Canadian Cordillera. *Tectonics*, **13**, 401–420.

—— & —— 1994*b*. Erosional exhumation of the British Columbia Coast Ranges as determined from fission-track ages of detrital zircon from the Tofino basin, Olympic Peninsula, Washington. *Geological Society of America Bulletin*, **106**, 1398–1412.

——, ——, RODEN, M. K. & ARCHIBALD, D. A. 1993. Time-integrated history of cooling and exhumation of the Coast Plutonic Complex, B.C., based on isotopic ages of detrital minerals. *Geological Society of America Abstracts with Programs*, **25**, 172–173.

GIGER, M. & HURFORD, A. J. 1989. Tertiary intrusives of the Central Alps: their Tertiary uplift, erosion, redeposition and burial in the south Alpine foreland. *Eclogae Geologicae Helvetiae*, **82**, 857–866.

GLEADOW, A. J. W., DUDDY, I. R., GREEN, P. F. &

LOVERING, J. F. 1986. Confined fission track lengths in apatite: a diagnostic tool for thermal history analysis. *Contributions to Mineralogy and Petrology*, **94**, 405–415.

GREEN, P. F., DUDDY, I. R., GLEADOW, A. J. W. & TINGATE, P. R. 1985. Fission track annealing in apatite: track length measurements and the form of the Arrhenius plot. *Nuclear Tracks and Radiation Measurements*, **10**, 323–328.

——, ——, LASLETT, G. M., HEGARETY, K. A., GLEADOW, A. J. W. & LOVERING, J. F. 1989. Thermal annealing of fission tracks in apatite: 4. Quantitative modelling techniques and extension to geological timescales. *Chemical Geology (Isotope Geosciences Section)*, **79**, 155–182.

GRIST, A. M., REYNOLDS, P. H. & ZENTILLI, M. 1990. Provenance and thermal history of detrital sandstones of the Scotian Basin, offshore Nova Scotia, using apatite fission track and $^{40}Ar/^{39}Ar$ methods. *Atlantic Geology*, **26**, 171.

HANSMANN, W. 1996. Age determinations of the Tertiary Masino–Bregaglia (Bergell) intrusives (Italy, Switzerland) – a review. *Schweizerische Mineralogische und Petrographische Mitteilungen*, **76**, 421–451.

HASEBE, N., TAGAMI, T. & NISHIMURA, S. 1993. Evolution of the Shimanto accretionary complex: a fission-track thermochronological study. *In*: UNDERWOOD, M. B. (ed.) *Thermal Evolution of the Tertiary Shimanto Belt, Southwest Japan: an example of Ridge–Trench Interaction*. Geological Society of America, Special Paper, **273**, 121–136.

HOLLISTER, L. S. 1982. Metamorphic evidence for rapid (2mm/yr) uplift of a portion of the Central Gneiss complex, Coast Mountains, B.C. *Canadian Mineralogist*, **20**, 319–332.

HORSTMANN, U. E. 1987. *The metamorphic evolution of the Damara Orogeny, Namibia, as deduced from K/Ar dating of detrital white mica from molasse sediments of the Nama Group* (in German). Goettinger Arbeiten zur Geologie und Palaeontologie, **32**.

HURFORD, A. J. 1986. Cooling and uplift patterns in the Lepontine Alps, south central Switzerland, and an age of vertical movement on the Insubric fault line. *Contributions to Mineralogy and Petrology*, **92**, 413–427.

——, FITCH, F. J. & CLARKE, A. 1984. Resolution of the age structure of the detrital zircon populations of two Lower Cretaceous sandstones from the Weald of England by fission-track dating. *Geological Magazine*, **121**, 269–277.

JOHNSON, C. & LONERGAN, L. 1996. Quantifying the exhumation history of Tertiary mountain belts from stratigraphic, provenance, and fission-track studies (abstract). *In*: *Abstracts for the International Workshop on Fission-track Dating, Gent 1996*. Geological Institute and Institute for Nuclear Sciences of the University of Gent, 61.

KAMP, P. J. J., GREEN, P. F. & TIPPETT, J. M. 1989. Tectonic architecture of the Mountain front–foreland basin transition, assessed by fission track analysis; fission track analysis reveals character of collisional tectonics in New Zealand. *Tectonics*, **8**, 169–195.

KASUYA, M. & NAESER, C. W. 1988, The effect of a-damage on fission-track annealing in zircon. *Nuclear Tracks and Radiation Measurements*, **14**, 477–480.

KOWALLIS, B. J., HEATON, J. S. & BRINGHURST, K. 1986. Fission-track dating of volcanically derived sedimentary rocks. *Geology*, **14**, 19–22.

MCGOLDRICK, P. J. & GLEADOW, A. J. W. 1977. Fission track dating of lower Palaeozoic Sandstones at Tatong, North Central Victoria. *Journal of the Geological Society of Australia*, **24**, 461–464.

MARANVILLE, R. E. 1993. Fission-track dating of detrital zircons from modern rivers in the Pacific Northwest: implications for the provenance of the Olympic subduction complex. *Green Mountain Geologist*, **20**, 6.

MULLER, J. E., SNAVELY, P. D., JR & TABOR, R. W. 1983. *The Tertiary Olympic Terrane, Southwest Vancouver Island and Northwest Washington*. Geological Association of Canada, Mineralogical Association of Canada, Canadian Geophysical Union, Field Trip Guidebook, Trip 12.

NAESER, C. W. 1976. *Fission-track Dating*. US Geological Survey Open File Report **76–190**.

——, ZIMMERMAN, R. A. & CEBULA, G. T. 1981. Fission track dating of apatite and zircon: an interlaboratory comparison. *Nuclear Tracks*, **5**, 65–72.

NAESER, N. D., NAESER, C. W. & MCCULLOH, T. H. 1989. The application of fission-track dating to the depositional and thermal history of rocks in sedimentary basins. *In*: NAESER, N. D. & MCCULLOH, T. H. (eds) *Thermal History of Sedimentary Basins, Methods and Case Histories*. Springer, New York, 157–180.

——, ZEITLER, P. K., NAESER, C. W. & CERVENY, P. F. 1987. Provenance studies by fission-track dating – etching and counting procedures. *Nuclear Tracks and Radiation Measurements*, **13**, 121–126.

PARRISH, R. R. 1983. Cenozoic thermal evolution and tectonics of the Coast Mountains of British Columbia 1: Fission-track dating, apparent uplift rates and patterns of uplift. *Tectonics*, **2**, 601–631.

PEREIRA, A. J. S. C., CARTER, A., HURFORD, A. J., NEVES, L. J. P. F. & GODINHO, H. M. 1996. Evidence for the unroofing history of Hercynian granitoids in central Portugal derived from Mesozoic sedimentary zircons (abstract). *In*: *Abstracts for the International Workshop on Fission-track dating, Gent 1996*. Geological Institute and Institute for Nuclear Sciences of the University of Gent, 86.

RENNE, P. R., BECKER, T. A. & SWAPP, S. M. 1990. $^{40}Ar/^{39}Ar$ laser-probe dating of detrital micas from the Montgomery Creek Formation, Northern California: clues to provenance, tectonics, and weathering processes. *Geology*, **18**, 563–566.

RODDICK, J. 1983. Geophysical review and composition of the Coast Plutonic Complex, south of latitude 55°N. *In*: RODDICK, J. A. (ed.) *Circum-Pacific Plutonic Terranes*, Geological Society of America, Memoir, **159**, 195–211.

ROHRMAN, M. & ANDRIESSEN, P. 1996. The relationship between sedimentary source and depositional area: a new challenge for AFT thermochronology (abstract). *In*: *Abstracts for the*

International Workshop on Fission-track Dating, Gent 1996. Geological Institute and Institute for Nuclear Sciences of the University of Gent, 94.

——, —— & VAN DER BEEK, P. 1996. The relationship between basin and margin thermal evolution assessed by fission track thermochronology: and application to offshore southern Norway. *Basin Research*, **8**, 45–63.

SCHAER, J. P., REIMER, G. M. & WAGNER, G. A. 1975. Actual and ancient uplift rate in the Gotthard region, Swiss Alps: A comparison between precise levelling and fission-track apatite age. *Tectonophysics*, **29**, 293–300.

SCHMID, S.M., BERGER, A., DAVIDSON, C., *ET AL.* 1996. The Bergell pluton (southern Switzerland, northern Italy) – overview accompanying a geological–tectonic map of the intrusion and surrounding country rocks (review). *Schweizerische Mineralogische und Petrographische Mitteilungen*, **76**, 329–355.

SEWARD, D. & RHOADES, D. A. 1986. A clustering technique for fission-track dating of fully to partially annealed minerals and other non-unique populations. *Nuclear Tracks and Radiation Measurements*, **11**, 259–268.

SPEER, J. A. 1980. Zircon. *In*: RIBBE, P. H. (ed.) *Orthosilicates*. Mineralogical Society of America, Reviews in Mineralogy, **5**, 67–112.

STOCK, J. & MOLNAR, P. 1982. Uncertainties in the relative plate positions of the Australia, Antarctica, Lord Howe, and Pacific Plates since the Late Cretaceous. *Journal of Geophysical Research*, **87**, 4697–4717.

STÜWE, K., WHITE, L. & BROWN, R. 1994. The influence of eroding topography on steady-state isotherms: application to fission track analysis. *Earth and Planetary Science Letters*, **124**, 63–74.

TABOR, R. W. & CADY, W. H. 1978. *The Structure of the Olympic Mountains, Washington – Analysis of a Subduction zone*. US Geological Survey, Professional Paper, **1033**.

TAGAMI, T. & DUMITRU, T. A. 1996. Provenance and thermal history of the Franciscan accretionary complex: constraints from zircon fission track thermochronology. *Journal of Geophysical Research*, **101**, 11353–11364.

TURNBULL, I. M. 1985. *Sheet D42AC and part sheet D 43 – Te Anau Downs Geologic map of New Zealand*, 1:50 000 (1 sheet) and notes, 1st edn. Department of Scientific and Industrial Research, Wellington.

——, URUSKI, C. I. *ET AL.* 1993. *Cretaceous and Cenozoic Sedimentary Basins of Western Southland, South Island, New Zealand*. Institute of Geological and Nuclear Science, Monograph, **1**.

TURNER, S. P., KELLEY, S. P., VANDENBERG, A. H. M., FODEN, J. D., SANDIFORD, M. & FLOETTMANN, T. 1996. Source of the Lachlan fold belt flysch linked to convective removal of the lithospheric mantle and rapid exhumation of the Delamerian–Ross fold belt. *Geology*, **24**, 941–944.

VANCE, J. A. 1989. Detrital kyanite and zircon: provenance and sediment dispersal in the Middle and Late Eocene Puget and Cowlitz groups, SW Washington and NW Oregon. *Geological Society of America, Abstracts with Programs*, **21**, 153.

WAGNER, G. A. & VAN DEN HAUTE, P. 1992. *Fission-Track Dating*. Kluwer Academic Publishers, Dordrecht.

——, MILLER, D. S. & JÄGER, E. 1979. Fission track ages on apatite of Bergell rocks from Central Alps and Bergell boulders in Oligocene sediments. *Earth and Planetary Science Letters*, **45**, 355–360.

——, REIMER, G. M. & JÄGER, E. 1977. *Cooling ages derived by apatite fission-track, mica Rb–Sr and K–Ar dating: the uplift and cooling history of the Central Alps*. Memorie degli Istituti di Geologia and Mineralogia dell'Universita di Padova, **30**.

YAMADA, R., TAGAMI, T., NISHIMURA, S. & ITO, H. 1995, Annealing kinetics of fission tracks in zircon: An experimental study. *Chemical Geology (Isotope Geosciences Section)*, **122**, 249–258

YIM, W. W. S., GLEADOW, A. J. W. & VAN MOORT, J. C. 1985. Fission-track dating of alluvial zircons and heavy minerals. *Journal of the Geological Society, London*, **142**, 351–356.

ZEITLER, P. K. 1985. Cooling history of the NW Himalaya, Pakistan. *Tectonics*, **4**, 127–151.

——, CHAMBERLAIN, C. P., & SMITH, H. A. 1993. Synchronous anatexis, metamorphism, and rapid denudation at Nanga Parbat (Pakistan Himalaya). *Geology*, **21**, 347–350.

——, JOHNSON, N. M., BRIGGS, N. D. & NAESER, C. W. 1982. History of uplifts in northwestern Himalayas using study of ages by fission tracks of detrital Siwalik zircons. *In*: *Symposium on Mesozoic and Cenozoic Geology in Celebration of the 60th Anniversary of the Geological Society of China, Beidaihe, China*. Geological Society of China, Beidaihe, 108–109.

——, ——, —— & —— 1986. Uplift history of the NW Himalaya as recorded by fission-track ages on detrital Siwalik zircons. *In*: JIQING, H. (ed.) *Proceedings of the Symposium on Mesozoic and Cenozoic Geology in Connection of the 60th Anniversary of the Geological Society of China*. Geological Publishing House, Beijing, 481–494.